DL/SCI/P 298E

preprint Daresbury Laboratory

DL/SCI/P 298E

SYNCHROTRON RADIATION AS A SOURCE TO STUDY TIME-DEPENDENT PHENOMENA

by

I.H. MUNRO, Daresbury Laboratory

Submitted to Proc. of the Nato Adv. Study Institute., St. Andrews, Scotland, March 1980.

SEPTEMBER, 1981

Science and Engineering Research Council
DARESBURY LABORATORY
Daresbury, Warrington WA4 4AD

SYNCHROTRON RADIATION AS A SOURCE TO STUDY TIME-DEPENDENT PHENOMENA

by

Ian H. Munro
Science and Engineering Research Council, Daresbury Laboratory,
Warrington WA4 4AD, U.K.

A number of important preliminary measurements have been carried out by groups in Orsay, Stanford and Hamburg and the scientific benefits of time domain measurements using synchrotron radiation have been discussed in several recent review articles[1-7]. These works have revealed that time resolved excitation and emission measurements can be carried out routinely with a resolution of at least 1 ns or better. For example, measurements have been made on the fluorescence decay of individual vibronic levels of small molecules, on emission from low quantum yield gases ($\sim 10^{-4}$) at low pressure ($\sim$ 1 torr) and on quenching mechanisms in rigid solutions. Pure rare gas solids and also mixtures have been studied extensively in an attempt to understand the kinetic processes associated with exiton formation. Also for the first time, quantum coherence effects have been seen in rare gases. Orientated atomic states can be produced by photoselection using polarised light for excitation and periodic fluorecence modulation can be seen in the presence of an external applied field. The treated data yields lifetimes, spins, multipolarities and "g" factors - even when the substates are unresolved in energy. More recently, photoselection of an individual residue within a protein with pulsed, polarised light has led to an understanding of the microenvironment within the large molecule and has enabled initial estimates to be made of the flexibility of such large structures as well as of their overall size and shape. The best time resolution obtained so far using conventional pulse techniques is about $\pm$ 50 ps and has been limited by the time response of the photodetectors used. The narrow

pulse width and the associated broad frequency spectrum (extending beyond 1 GHz) from storage ring sources has led to the study of phase shift and modulation techniques at a number of different frequencies. Preliminary results have revealed that in the frequency domain, measurements corresponding to times of the order of a few ps can be measured. It is highly probable that, in the future, time domain measurements will be improved to give a resolution of about 1 ps and will be extended to include excitation over an extensive range of wavelengths in the VUV and X-ray regions.

Synchrotron Radiation as a Source for Spectroscopy

The general properties of a storage ring as a source for spectroscopy are well illustrated by reference to the Synchrotron Radiation Source (SRS) completed in June 1980 and now operational at the Science and Engineering Research Council, Daresbury Laboratory, in the UK[8]. The SRS is a 2 GeV electron storage ring designed to maintain a useable circulating current of electrons of up to 1 A for periods of at least eight hours. The initial maximum current will be restricted to 0.37 A until sufficient additional radio frequency power has been installed to permit operation at its design current of 1 A.

The electrons are confined within the storage ring by circular array of sixteen electromagnets shown in fig.1. The magnetic field associated with each of these dipole bending magnets defines the electron momentum, P, (and therefore the particle energy) according to the relationship $P = BeR$, where B, e, R are the magnetic field strength, electron charge and the electron orbit radius respectively. The acceleration experienced by each electron is directed radially inwards and results in the production of electromagnetic radiation (synchrotron radiation). To a station-

ary observer looking along a beam line tangentially into the storage ring, the circulating electrons will appear to be approaching at a speed extremely close to the speed of light (approximately to within one part in 10^6 of c at 2 GeV). The relativistic consequences of this very high speed motion of the source are impressive. First, the peak power in the frequency spectrum of the emitted radiation is enormously "blue-shifted" from the microwave region into the x-ray region and, secondly, radiated power is almost totally confined to a small forward cone of about $\frac{1}{20}$ degree angle. The exact relationships betwen the spectral characteristics of the source and the parameters of the storage ring have been calculated, measured and extensively described[9,10].

Figures 2 and 3 summarise the source properties. The synchrotron radiation spectral continuum shown in fig.2, is useful for spectroscopy over about 8 decades of frequency with an intensity peak at around 4 Å. X-ray experiments may typically accept 1 mrad of beam (equivalent to 3.4 minutes of arc) and an upper angular limit would probably be given by 100 mrad (about 5°) for experiments at longer wavelengths in the visible and infrared regions. The average maximum power radiated over <u>all</u> wavelengths is around 40 W per mrad. The "wiggler" is a specially constructed high magnetic field array of three magnets designed to shift the entire spectral distribution to shorter wavelengths for x-ray scattering experiments which require particularly "hard" x-radiation (see fig.2). The synchrotron radiation source brightness is defined by the source size (the observed cross section of the electron beam), the source intensity (measured from fig.2) and by the beam divergence (defined by the curve given in fig.3). The emergent beam is almost completely collimated at short wavelengths and has a low vertical divergence of about 5 mrad in

the visible region. The electron beam source size may differ between different storage rings and between different positions within any given ring. In all storage rings the horizontal beam dimension is normally greater than the vertical dimension. At the SRS, the horizontal and the vertical source sizes lie within the extreme values of 14.8 mm to 2.6 mm and 0.35 mm to 3.3 mm respectively. With care, and money for additional focusing magnets, the source dimensions at individual points on orbit may be diminished. The vertical size of the beam could be as small as 0.05mm.

Radiation from the SRS is also predominantly linearly polarised with the electric vector horizontal i.e. parallel to the orbit plane of the storage ring. As the out-of-plane viewing angle is increased, the polarisation changes from linear to elliptical and becomes circularly polarised at very large out-of-plane angles, although here the intensities of the two components asymptotically tend to zero. The average degree of polarisation is clearly dependent on the beam divergence for any particular wavelength. For hard x-rays, where the emergent beam is highly collimated the radiation will therefore be almost totally polarised. In the visible region the degree of polarisation is around 75% when radiation is collected over all vertical angles[8].

<u>Time Modulation of Synchrotron Radiation</u>

The circulating beam within a storage ring continuously loses energy by the emission of synchrotron radiation and by scattering of electrons out of the beam following collisions with residual gas molecules. The electron beam is maintained by supplying power via one or more resonant cavities which operate at some selected radio frequency, usually in the range between 10 MHz and 500 MHz. The dynamics of the particles (e^-) in

any storage ring are primarily defined then by the balence between particle excitation resulting from the emission of quanta of synchrotron radiation and the longitudinal focusing and damping associated with the magnetic lattice and radio frequency drive.

Obviously, the time modulation impressed on the spectral characteristics of synchrotron radiation is established by the modulation of the electron beam current passing through the observed synchrotron radiation source points around the orbit. Furthermore, all of the time characteristics of the source - the pulse shape, frequency and jitter - will be absolutely identical for all emitted wavelengths. This source characteristic is of extreme importance when the time response of the detector and its associated electrons have to be unfolded from the measured data.

Since electrons will be accelerated only when in phase with the accelerating radio frequency field, it is clear that a storage ring will, in general, contain a train of electron bunches separated by the period of the r.f. field. Each storage ring operates at a fixed frequency (since the electron speed is approximately constant) and therefore the ring can contain an integral number of bunches from one to a maximum number (the "harmonic number", N), defined by the ratio of the circulation period around the ring to the period of the accelerating r.f. field. The ring period is given by the ratio of ring circumference to the speed of light and for the very largest (and therefore most expensive) accelerators, has a value of about one microsecond. The maximum radio frequency used for acceleration is restricted to 500 MHz by the commercial availability of high power, high frequency klystrons which are extremely costly, and by technical problems associated with transmission of the r.f. power through a window into the acceleration cavity in the storage ring which

must be maintained at a very low pressure ($\lesssim 10^{-9}$ torr). An indication of the wide variety of existing storage ring source parameters is shown in Table I where the lowest harmonic numbers result from using a low radio frequency for electron acceleration in a ring of small size. The information is tabulated in order of increasing E_c which is defined to be the photon energy value corresponding to the peak of the spectral intensity curve. To obtain useful amounts of hard x-radiation, that is, radiation which can pass through a Be window into air, the stored beam energy must typically be 2 GeV or more. Of course, power radiated at the shortest wavelength can be enhanced using a wavelength shifter or wiggler (see fig.2).

N, the harmonic number or the maximum number of bunches within a storage ring may vary greatly from ring to ring (see Table I). However, the majority of storage rings have been designed so that they can function perfectly reliably with a single bunch only in the storage ring. This type of operation (often called the "single bunch mode") is achieved usually at the expense of a reduction in the number of stored electrons. Whereas in "multi-bunch" modes or the "filled" mode of operation most of the storage rings listed in Table I will maintain a circulating current of from 100 mA to 1 A, in the "single bunch" mode the circulating current is unlikely to exceed ~ 50 mA. The actual length of the electron bunch in a storage ring is related to the frequency and amplitude of the acceleratting field. Bunch lengths have been measured directly for a relatively small number of storage rings but the calculated natural bunch lengths (in the absence of other bunch lengthening effects) lie between 50 to 100 cm for ADONE and TANTALUS to around 5 cm for the majority of the 500 mHz rings. The lengths correspond to excitation light pulse widths (between

Table 1

Some parameters of storage rings which are used as synchrotron radiation sources

	E_o (GeV)	R (m)	E_c (keV)	T_o (ns)	N	T_{rf} (ns)
SURF (Washington, USA)	0.25	0.83	0.041	17.5	2	8.8
TANTALUS (Stoughton, USA)	0.24	0.64	0.048	31.4	1	31.4
INS-SOR (Tokyo, Japan)	0.3	1.1	0.054	57.8	7	8.3
ACO (Orsay, France)	0.54	1.11	0.31	73.5	2	36.7
BROOKHAVEN (USA) VUV Ring	0.7	1.9	0.40	170.3	9	18.9
BESSY (Berlin, West Germany)	0.75	1.8	0.52	208.3	26	8.0
					104	2.0
VEPP 2M (Novosibirsk, USSR)	0.67	1.22	0.54	59.9	20	3.3
ALADDIN (Stoughton, USA)	1.0	2.08	1.1	295.0	15	19.7
ADONE (Frascati, Italy)	1.5	5.0.	1.5	349.7	3	111.7
DCI (Orsay, France)	1.8	3.82	3.4	316.4	8	39.5
SRS (Daresbury, UK)	2.0	5.55	3.9	320.5	160	2.0
PHOTON FACTORY (Tsukuba, Japan)	2.5	8.33	4.1	598.8	285	2.1
BROOKHAVEN (USA) X-ray ring	2.5	6.8	5.1	568.2	30	18.9
DORIS (Hamburg, West Germany)	3.5	12.1	7.8	961.5	481	2.0
SPEAR (Stanford, USA)	4.0	12.7	11.1	781.2	279	2.8
CESR (Cornell, USA)	8.0	88	12.8	2222.0	1111	2.0
VEPP-4 (Novosibirsk, USSR)	7.0	29	26.0	1250.0	227	5.5

half maximum points) of from ~ 2 ns to $\lesssim$ 200 ps.

Synchrotron Radiation Source Geometry

The ideal pulsed source for time resolved experiments would be a train of extremely narrow pulses separated by long but adjustable time periods. Such is the case for a large storage ring where the pulse width may be ~ 100 ps with an inter-pulse period of ~ 1 μs. In a storage ring, the optical source is the radial cross section of the electron beam at that tangential orbit point which lies on the optic axis of the experiment. In order to increase the amount of light falling on any experiment, the horizontal angular spread of radiation collected from the ring obviously is to be increased. Since the source (circulating electrons) actually moves, this then will add time spread to the synchrotron radiation pulse width. Figure 4 illustrates how the additional time dispersion arises. For any apparent axial tangent point T, a radiation collection aperture of 2 θ will permit radiation from all points on the arc ATB to be collected in any chosen observation plane.

The path length of the electrons and photons to the point of observation is given by

$$x(\theta) = \frac{L}{\cos \theta} + R\,(\theta - \tan \theta) \ .$$

The pulse broadening, Δt, is given by

$$\Delta t(\theta) = \frac{1}{c}\left[x(\theta) - 1\right] \ .$$

In a large storage ring where R may be 10m or more, Δt is approximately 1 ps for θ ~ 10 mradians and the time dispersion effect can be neglected. Nevertheless the length and curvature of the source may still cause imaging problems, particularly if any focusing collection mirrors are used

near grazing incidence. In principle the problem could be eliminated for any angle if the image plane (or detector) is shaped and curved to follow an isochronous surface. For a flat image plane and a large storage ring (R ~ 10 m), the time dispersion associated with geometry will only become important for very large collection angles of the order of 100 milliradians when Δt > 20 ps.

Time Resolved Experiments using Synchrotron Radiation

It is valuable to identify the different kinds of physico-chemical information associated with measurements made in different time ranges and alongside these ranges, to identify the limitations in timing techniques available at present.

Table II reveals that the goal of the synchrotron radiation spectroscopist must be to include, along with all the other spectroscopic properties of the source, the ability to carry out experiments within the picosecond and ultimately the sub-picosecond time domain. It is important to note that molecular motions in the picosecond region which can be measured in the time domain also may be accessible to the synchrotron radiation spectroscopist by the direct observation of molecular rotational or vibrational absorption effects in the submillimetre region.

It is clear from Table I that, for the majority of storage ring sources, experiments will be confined to time studies significantly shorter than 1 μs as a consequence of the upper limit in size of a storage ring, which corresponds roughly to a maximum inter-pulse excitation period of one or two microseconds. The minimum inter-pulse period with a filled ring such as the SRS at Daresbury Laboratory is approximately 2 ns (corresponding to 500 MHz) and therefore one aim of this article is to identi-

Table II

Time range(s) (equivalent time length)	Physical Phenomena	Timing Techniques
10^{-15}s (femtosec) (3000 Å)	photon absorption electron emission	
10^{-12}s (picosec) (0.3 mm)	molecular rotations molecular vibrations electron transfer	laser pulse width streak camera high frequency phase shift in modulation
	exciton migration energy transfer collisions in gases and liquids	storage ring pulse width coincidence techniques real time studies
10^{-9}s (nanosec) (30 cm) 1 GHz	fluorescence molecular tumbling in solution bimolecular reactions	flash lamp duration
10^{-6}s (microsec) (300 m)	phosphorescence	NMR line shape EPR
10^{-3}s (millisec) (300 km)		

fy the best probable time resolution which could be achieved in the sub-nanosecond domain.

The properties of electron synchrotrons as synchrotron radiation sources will not be discussed except to say that, as a consequence of their basic electron/injection extraction frequency of about 50Hz, they can and have been used as sources for time resolved studies in the millisecond region[11,12].

Pulsed Excitation Measurements

In the majority of e^+e^- colliding beam storage rings used for elementary particle physics studies, the count rates around each interaction region (that is, the experimental luminosity) is of primary importance and there have been no attempts to minimise the bunch length in particular.

In some accelerators, for example in SPEAR at Stanford, r.f. acceleration cavities operating at some low harmonic of the fundamental have been used in an attempt to shape the particle bunch. Nevertheless, although particle bunches can be shaped and reduced in length, all existing storage rings, including those first few storage rings dedicated to synchrotron radiation research, accelerate bunches which are unnecessarily and unreasonably long ($\tilde{>}$100 ps), at least from the point of view of time resolved molecular spectroscopy.

The first timing experiments conducted at storage ring facilities showed the circulating electron bunch, and therefore the radiation excitation pulse to be approximately Gaussian in profile and independent of bunch current[13]. This result is predicted by a classical model of the equilibrium bunch length in a storage ring which includes interactions between the geometry of the storage ring magnetic lattice, amplitude and frequency of the r.f. accelerating field and the electron energy fluctuations associated with synchrotron radiation emission[14].

This paper will not include a detailed discussion of the specific requirements of each technique used for short time measurements. However, a prerequisite of all repetitive timing measurements is that of source stability. In the case of sampling oscilloscope studies, for example, the source pulse shape and amplitude must remain fixed for the duration of the experiment, while for coincidence studies (i.e. for "single photon counting") it is the excitation pulse shape which must remain time invariant. In these respects storage ring sources are ideal for timing measurements in the region from nanoseconds to tenths of nanoseconds. A storage ring will provide an invariant pulse shape of width between 100 ps and 1 ns with a high and extremely stable pulse repetition frequency

over periods of many hours. The peak amplitude of the pulse will diminish as the stored current in the ring gradually reduces due to residual gas scattering with a beam half life in the SRS of around eight hours. and which is monitored continuosly by the storage ring operators.

An illustration of the good statistical quality of data which can be obtained using commercially available modular electronics for photon counting studies is given in fig.5a,b,c. The measurement of the time dependence of the fluorescence anisotropy of individual amino acids residues in a biopolymer may be of considerable importance in relating the structure and the function of large molecules such as proteins[15]. Ideally, these experiments should be carried out in conditions similar to those in the physiological environment and this usually implies a low protein concentration of micromolar or less in aqueous solution. Anisotropy measurements with small statistical errors are particularly difficult to make because the anisotropy decay curve A(t) is defined to be the difference at any time between the intensities of two fluorescence emission components with orthogonal polarisation. A further problem arises because of the extreme sensitivity of the measurement to the presence of incident (excitation) light scattered directly into the detector without alteration in the direction of polarisation. The experiment demands an intense light pulse with minimum possible duration. The excitation pulse must be linearly polarised, tuneable in wavelength and with a variable and narrow wavelength spread. Since the number of fluorescent residues and their quantum yield may be small, a high repetition rate is required from the source in order to complete data taking before any photosensitive or other changes can take place in the sample. These requirements are extremely well matched to synchrotron radiation from storge ring sources. In fig.5, the

results show a SPEAR excitation pulse (f.w.h.m. ~ 120 ps) observed with an RCA 8850 photomultiplier giving an overall excitation function of about 650 ps f.w.h.m. shown in fig.5a. Raw anisotropy decay curves are shown for tryptophan in n-acetlytryptophanamide and these display a rotational correlation time reducing from 16 ns at 1400 cP to about 50 ps at 4 cP in a series of glycerol/water mixtures. The measured data in fig.5c is shown alongside theoretical curves for a range of correlation times (fig.5b) folded with the excitation function used shown in fig.5a. At the very shortest correlation times, the information is extracted primarily from the amplitude of the decay rather than its slope - hence the need for a significantly reduced excitation function. When a good least squares fitting procedure is applied, then a time resolution of at least ± 50 ps should be achievable for a maximum of three components both in the fluorescence and the anisotropy decay times.

Prospects for Bunch Length Reduction

In the majority of time resolved studies using synchrotron radiation sources, the excitation function has been determined primarily by the response time of the detector. In the immediate future, the use of single or double microchannel plate detectors, or of special design, low gain, crossed field photomultipliers will offer an improvement in time resolution by about a factor of three[16,17]. On the other hand, the use of a streak camera or of phase sensitive detection at high frequency necessitates that the electron bunch length itself (and therefore the excitation pulse deviation) must be of a similar order and as close as possible to the time range of interest, that is to say about 10 ps (see Table II).

With the intention of reducing the electron bunch length in a storage ring below about 3 cm (corresponding to 100 ps) at least one study has been

carried out on the dependence of bunch length on the storge ring parameters[18] and a detailed study for minimum bunch length has been incorporated within the design of the new storage ring BESSY in Berlin which is due for completion in 1982[19].

The classical model of an electron bunch in a storage ring yields a Gaussian bunch intensity profile. There will then arise an electromagnetic interaction between the electron bunch and its metal containment vessel and perhaps a further interaction back on the electron bunch itself. In a real storage ring, the electron bunch can be subject to a variety of perturbations which may create instabilities within the bunch and distort its shape in an unsystematic way. Instabilities of this kind can play a part in current dependent bunch lengthening although an attempt is made to minimise such difficulties by careful design and control of the complex coupling impedance of the ring as defined by the internal surfaces and apertures within the vacuum vessel. In a real ring the phase of the electron bunch with respect to the r.f. field will change as the circulating current is altered in a manner defined by very many different storage ring parameters.

In the absence of bunch lengthening effects the natural bunch length in a storage ring (usually expressed as σ_z, i.e. one standard deviation in length) is given by

$$\sigma_z \sim \text{constant} \cdot \sigma_\varepsilon \sqrt{\frac{\alpha T_o}{E_o \dot{V}}}$$

where σ_ε is the energy spread in the particle bunch, α is the momentum compaction factor for the storage ring, T_o is the bunch revolution period, E_o is the ring energy and $\dot{V} = dV/dt$ is the time derivative of the r.f. acceleration voltage. With some approximations, the f.w.h.m. of the radiation

pulse ($\Delta t \doteq 2.4\ \sigma_z/c$) can be shown to depend on the product $E^{3/2}.V^{-1}.T_o^{1/2}.\alpha^{1/2}$. Therefore the bunch length will be shortest at the lowest energy and with the highest total r.f. voltage applied. The bunch length will diminish as the radio frequency used for acceleration is increased and as the momentum compaction factor for the ring is reduced. There are constraints on the minimum value for the ring energy such as the maintenance of a reasonable Touschek lifetime at injection and the spectroscopic requirements of the users. There are also limits to the maximum value of $\dot{V}$ set by the maximum frequency (about 500 MHz) and maximum overvoltage which can be supported by each r.f. cavity window which separates the ring vacuum from the r.f. klystron power source.

The reduction in bunch length in storage rings of the future - such as BESSY - is to be achieved primarily by a reduction in the momentum compaction factor of the storage ring using special ring magnet optics which also provide an exceedingly small beam cross section and hence very high source brightness[20]. Figure 6 illustrates some of the problems which can be associated with short bunches in the SPEAR (Stanford) storage ring. Individual bunch intensity profile measurements were made using an Imacon 600 streak camera by viewing the visible light emitted from a single bunch passing through a selected orbit point[18]. The storage ring parameters were altered from 2.18 GeV and 0.88 MV to 1.5 GeV and 3.3 MV yielding an anticipated reduction in pulse width from 310 ps to 61 ps. However, the actual current in the bunch was found to modify the bunch shape. With circulating beam currents of from 8 to 10 mA, "turbulence" in the bunch occured in association with a bunch lengthening effect as a random, unsystematic modulation of the particle distributions in the bunch. This is shown clearly for the wider pulse shown in fig.6. Streak camera pic-

tures of a particular bunch taken at different times would reveal a similar overall profile with dissimilar amplitude and frequency modulation across the bunch. At low circulating current values below the "turbulence" threshold, individual bunches were found to have very similar amplitude and frequency modulation across the bunch profile at different times. The minimum f.w.h.m. value obtained was 55 ps at 3.3 MV, 1.5 GeV and 2.15 mA. The origin of the high frequency modulation of the envelope (of about 50 GHz) has not yet been explained (see fig.6) and was not related to any oscillation modes of the bunch, which were simultaneously measured using an antenna in the vacuum chamber and a Tektronix power spectrum analyser. Preliminary streak camera observations of bunch shape in DORIS (Hamburg) have not observed such modulation within their bunch[21]. There is therefore reason to suppose that the BESSY (Berlin) ring may be able to maintain a bunch length (σ_z) of about 1 mm corresponding to a minimum excitation pulse fwhm of $\tilde{>}$ 10 ps. However, this will be possible only if collective effects within the bunch are negligible as the stored current tends to zero. These conditions should apply for stored currents of roughly 1 mA[19,20].

Measurements in the Frequency Domain

A storage ring can produce a series of extremely narrow light pulses separated by a repetition period whose maximum value can be selected to be the ring period T_o, and whose minimum value will be defined by the period of the r.f. accelerating field, $T_{r.f.}$ Figure 7 illustrates the situation (i) for a storage ring in the "single bunch" mode, (ii) for a storage ring ring "filled" and (iii) to represent the decay of fluorescence intensity from a sample normalised to the excitation pulse in (ii). When "real time" or coincidence measurements, are carried out, the functions I(t) and R(t)

are measured independently and then used to compute a true fluorescence decay or an anisotropy decay function F(t). The measured functions I(t) and R(t) are related to the true fluorescence decay function (F(t)) which is to be determined by the convolution integral,

$$R(t) = \int_0^\infty I(t)\ F(t - t')\ dt' \ .$$

A variety of procedures can be used to unfold the excitation function from the measure data and are discussed elsewhere in this volume. A rule-of-thumb would indicate that for statistically good quality data, decay times can be accurately extracted down to values of about one tenth of the f.w.h.m. time spread of I(t). Figure 8 schematically shows the Fourier transform of the pulses in fig.7(i). The transform consists of a set of harmonics (of width δn) related to the r.f. used for the acceleration and to the bunch dynamics within the storage ring. The fundamental (minimum) frequency is determined by $n = T_{rf}^{-1}$ (or T_o^{-1} if the storage ring is used in the single bunch mode). The amplitude envelope for the harmonics in the frequency spectrum is defined by the shape and width of the function I(t). If the pulse shape is Gaussian then the harmonic envelope will be Gaussian also. The spectral purity of the harmonics in the transform is established by the stability of the electron bunch and the stability of the storage ring r.f. system. Any instabilities will appear as sidebands about the harmonics. For large instabilities and high harmonic number, the sidebands may be even larger than the actual line. When a fluorescence decay function R(t) is measured, its Fourier transform will reveal the same set of harmonics n_i of width δn but whose amplitude profile has been modified to correspond to the extended pulse shape of R(t) compared with the excitation pulse I(t). The excitation transform and fluorescence transforms

are contrasted in fig.8. However, not only is the amplitude envelope modified, but each successive harmonic contained within the transform contains a phase shift where the actual phase angle between identical harmonics in I(t) and R(t) increases progressively with increasing harmonic number. When a phase comparison is made between the same harmonic in the fluorescence and excitation signals, the maximum phase difference will therefore be observed at the highest measurable frequency.

Figure 9 presents raw data obtained under identical operating conditions from an RCA 8850 photomultiplier tube. In real time, the detector produces a pulse width of about 2 ns f.w.h.m. (shown in fig.9(i) when viewing the 200 ps light pulse from SPEAR operating in the single bunch mode with a repetition frequency, (T_o^{-1}), of 1.28 MHz. The transform of this impulse response - or, at least, an indication of the transform profile - can be provided using a power spectrum analyser which will identify the signal power at each frequency but will not incorporate any signal phase information. Figure 9(ii) shows the power spectrum from the RCA.8850 photomultiplier tube. The resolution is inadequate on the scale presented to reveal that the power envelope outlines the response (efficiency) of the tube over a broad range of harmonies of the 1.28 MHz fundamental. Even at 358 MHz, the signal/noise ratio of the 280^{th} harmonic of about 16 dB. The pulse width in this experiment was approximately 200 ps which would correspond, for a pulse of Gaussian shape, to a power spectrum with frequency width of 3.6 GHz or a response down to half the central peak value at 1.8 GHz. Obviously in the case of fig.9(ii) the power/frequency spectrum is much narrower than 1.8 GHz and must, therefore, be almost totally characteristic of the detector response alone. This affords a very simple and exact manner in which to measure the temporal response of

any photon detector[23].

Phase and Modulation Fluorometry

The wide range of harmonics associated with the radiation from each storage ring obviously enables use of narrow band pass (high"Q") r.f. filters to select any suitable frequency for study. The purpose of phase or modulation sensitive experiments is then to compare, usually via a neutral scatterer as a double reference, the relative phase delay (θ) and the ratio (m) of the modulation amplitudes of reference (excitation) and sample signals. If a sample fluorescence decay function can be represented by an exponential function (lifetime τ) then

$$\tan \theta = n_i \tau ,$$

$$\text{and} \quad \cos \theta = m = \frac{1}{\sqrt{1 + n_i^2 \tau^2}} ,$$

where n_i can be the fundamental or any harmonic of the pulse repetition frequency.

Using standard electronics, it is possible to make a phase comparison between two signals of rather low amplitude (>20μv) and of high frequency (~ 500 MHz) to within perhaps 0.1°, which would correspond to a sample fluorescence lifetime of only 600 fs (or 0.6 ps!)

There are a great many ways in which such a phase comparison can be made and one example of a phase shift apparatus is shown in fig.10. Using that apparatus, the transmission time of monochromatic radiation through an optically flat slab of 1.5 cm of fused SiO_2 was measured to an accuracy of ± 2 ps[7,24]. The effective "time thickness" of the slab revealed a spectral dependence which could not be explained by refractive

index changes, interference or multiple reflection phenomena. The synchrotron radiation pulse which passed through the slab was detected by a photomultiplier tube, amplified and then filtered by a SAW (surface acoustic wave) filter. In this case the 35^{th} harmonic (44.817 MHz) of the SPEAR orbit frequency was further amplified and fed to the signal input of a phase sensitive lock-in amplifier (see fig.10). The high frequency reference signal is obtained from the storage ring power source via a similar SAW filter. The signal phase (θ) was measured to be the ratio of the "in phase" (I) and quadratic (Q) outputs from the "lock-in" amplifier, where $\tan \theta = Q/I$. In bench tests without a storage ring, phase measurements of this kind can be made easily to correspond to subpicosecond transit times. Consequently, since the standard deviation of the data was approximately $\pm$ 2 ps, it is possible that phase fluctuations - from the storage ring source introduced this time resolution limit - at least in the case of SPEAR.

It should be noted that for <u>any</u> harmonic frequency n_i, the propagation delay through a sample may be measured as a phase shift $\Delta\theta$ given by $\Delta\theta = n_i \Delta t$. Further, following reflection of incoherent monochromatic light by an optical surface the time pulse envelope must remain unchanged. Therefore every harmonic frequency n_i will be shifted in phase by the amount of the optical phase shift $\Delta\theta$ and thus extremely sensitive phase shift ellipsometry is possible using the higher modulation frequencies from a storage ring. Phase shift studies have been undertaken so far only at SPEAR (Stanford) and ACO (Orsay) but it is clear that a wide range of heterodyning techniques using frequency mixing, or sample or detector motion, can be exploited to give accurate results in the picosecond region at frequencies up to perhaps 1 GHz.

<u>Conclusions</u>

Storage ring sources clearly promise the ultimate possibility of conducting time dependent spectroscopic studies at all wavelengths with a time resolution of about 1 ps. In the pursuit of that goal it is obviously necessary to continue to develop high gain detectors with a frequency response extending well into the GHz range[25]. The possibility of incorporating spatial resolution and good time resolution in devices such as microchannel plate arrays will also become important in the detection of electrons and photons. In addition, the storage ring source must be used with high throughput monochromators which give good wavelength resolution, very low scattered light levels, which are optically matched to the source and retain the polarisation properties of synchrotron radiation. The accumulated data should preferably be processed on-line using a technique such as iterative reconvolution with residuals. It is important when using a storage ring source - particularly if it is operating selectively for timing experiments in the single bunch mode - to identify the quality of the data as rapidly as possible because of the competition between different users for experimental time on the machine.

It is important also to recognise the many similarities between synchrotron radiation and laser sources - the most obvious differences being the continuous spectral range of synchrotron rdiation into the x-ray region and the coherence and the exceedingly high peak radiation powers from lasers. Table III (from[6]) represents a broad comparison between a variety of parameters associated with conventional sources, lasers and synchrotron radiation.

The pulsed properties of synchrotron radiation are being applied extensively to develop other important techniques including electron energy

Table 3

Source comparison

	Storage ring sources	Pulsed lasers	Flash and discharge lamps
Spectral range	Tuneable from submillimetre to x-ray (from 0.1 nm to 1 cm).	Tuneable over small ranges in visible and UV. Many lines in the infrared. Few lines in VUV and soft x-ray region.	The range from 1cm to characteristic x-ray lines can be only partially covered and many different source types are needed.
Pulse intensity (numbers of photons in 0.1% $\Delta\lambda/\lambda$)	$< 10^9$ perhaps up to $\gtrsim 10^{12}$ using undulator devices.	$>10^{10}$ in 1 ps for pulse width of 10 cm^{-1}.	usually low, $< 10^6$ at best.
Minimum pulse duration (f.w.h.m.)	typically 100 ps, anticipate 20 ps, identical at all wavelengths.	0.2 ps at best for selected medium. Wavelength dependent.	usually > 1 ns. Extremely variable as a function of wavelength.
Pulse repetition rate	~ 1 MHz to few GHz, extremely stable, totally modulated.	d.c. to ~ 100 MHz, not stable for long periods, partially modulated.	d.c. to $\lesssim$ 100 MHz, can be stable for limited periods, partially modulated.
Pulse shape and amplitude	Stable and predictable.	variable.	variable.
Source size and divergence	~ 1 mm^2 (anticipate 50 μ × 150 μ) $\lesssim$10 milliradians.	$\gtrsim$1 mm^2 $\gtrsim$5 milliradians	few mm^2 isotropic
Other properties	Can be totally linearly polarised Incoherent	usually linearly polarised. Coherent	Usually unpolarised. Incoherent

analysis and ion mass/energy analysis using time of flight techniques studies of coherence lengths and times using correlation techniques and the separation of nuclear and electron scattering in Mössbauer experiments using fast gating methods[10].

Future opportunities are tentatively presented in the diagram given in fig.11,[28]. Synchrotron radiation sources are, at present, the key to the extension of subnanosecond timing studies into the vacuum ultraviolet and x-ray regions. The principal fast photon detector device which can match the temporal properties of a picosecond source is a streak camera[25,26]. This device or a modification of it, can be used any wavelength from the visible to the x-ray region. Where sufficient signal intensity is available it will be used in a "single shot" mode. When few photons only are available, the streak camera can be operated synchronously[26,27]. With the development of a suitable photodiode array in combination with image intensification, a streak camera could be driven synchronously with a storage ring to measure accumulated decay profiles on the basis of only a few emitted photons per excitation event. Experiments of this type will no doubt be conducted in the near future as the first generation of purpose-built, dedicated storage ring sources come into operation.

In the slightly longer term, the use of extensive arrays of bending magnets may yield a further enhancement in radiated intensity of from M to M^2 where M is the number of bending magnets in the device. Since M could be as large as 10^2 (perhaps 10^3?) the increase will be from 10^2 times for wiggler magnet arrays to up to 10^4 times for an undulator device[29,30]. Should it prove possible to develop free electron laser technology beyond the present rudimentary state-of-the-art, then within

perhaps five years one could anticipate high power pulsed and continuously tuneable free electron laser sources yielding coherent radiation with narrow line width into the VUV and possibly even the soft x-ray region[31].

References

1. R. Lopez-Delgado, A. Tramer, I.H. Munro, Chem. Phys. 5, (1974) 72-83.
2. R. Lopez-Delgado, Intern. Coll. of Appl. Phys. 1, (1976) 63-124. Nato Advanced Study Institute, Alghero, Italy, Eds. A.N. Mancini and S.F. Quercia.
3. R. Lopez-Delgado, Nucl. Instrum. Meths. 152, (1978) 247-253.
4. K.M.Monahan, V. Rehn, Nucl. Instrum. Meths. 152, (1978) 255-259.
5. U. Hahn, N. Schwentner, G. Zimmerer, Nucl. Instrum. Meths. 152, (1978) 261-264.
6. I.H. Munro and A.P. Sabersky, Chapter 9 in "Synchrotron Radiation Research", Eds. H. Winick and S. Doniach. (Plenum Press, New York, 1980).
7. V. Rehn, Nucl. Instrum. Meths. 177 (1980) 193-206.
8. K.R. Lea and I.H. Munro, The Synchrotron Radiation Source at Daresbury Laboratory, Daresbury Laboratory Report DL/SCI/P ??? (1980).
9. "Topics in Current Physics - Synchrotron Radiation; Techniques and Applications", Ed. C. Kunz, (Springer-Verlag, Berlin, 1979).
10. Chapters 1-3 in "Synchrotron Radiation Research", Eds. H. Winick and S. Doniach (Plenum Press, New York & London, 1980).
11. S.S. Hasnain, T.D.S. Hamilton, I.H. Munro and E. Pantos, Daresbury Laboratory Report, DL/SRF/P007, (1977).
12. J.C. Haselgrove, A.R. Faruqi, H.E. Huxley and U.W. Arndt, J. Phys. E: Sci. Instrum. 10, (1977) 1035-1040.
13. R. Lopez-Delgado, J.A. Miche, B. Sipp and H. Zyngier, Nucl. Instrum. Meths. 133, (1976) 231-236.
14. M. Sands, "The physics of electron storage rings", Stanford Linear Accelerator Center Report, SLAC-121, (1970).
15. I.H. Munro, I. Pecht and L. Stryer, Proc. Natl. Acad. Sci. USA, 76, (1979) 56-60.

16. N. Schwentner, U. Hahn, D. Einfeld and G. Mulhaupt, Nucl. Instrum. Meths. 167, (1979) 499-503.

17. B. Leskovar and C.C. Lo, Lawrence Berkeley Laboratory Report, LBL-6456, (Oct.1977).

18. K.M. Monahan, I.H. Munro, L.F. Chase, B.A. Watson, M.Donald and J. Sheppard, Stanford Synchrotron Radiation Laboratory Users' Meeting (1979), and to be published.

19. D. Einfeld, BESSY Technical Report, TB-26/1980, (May, 1980).

20. D. Einfeld and G. Mülhaupt, BESSY Technical Report, TB-13/1979, (June, 1979)

21. N. Schwentner, HASYLAB, private communication.

22. P.L. Csonka, Stanford Synchrotron Radiation Laboratory Report, SSRL-79/04, (July 1979).

23. A.P. Sabersky and I.H.Munro, 85-88, in "Picosecond Phenomena", Eds. C.V. Shank, E.P. Ippen and S.L. Shapiro, Chem. Phys. Ser. 4, Sprinter-Verlag, Berlin, (1978).

24. V. Rehn, K.M. Monahan and I.H. Munro, Int. Conf. Quantum Electronics, Boston, 23-26 June 1980.

25. F. Heisel, J.A.Miehe and B.Sipp, Ann. Phys. Fr. 4, (1979) 331-370.

26. J.R. Taylor, M.C. Adams and W. Sibbett, Appl. Phys. 21, (1980) 13-17.

27. B. Quinn, J.A. Miehe, B. Sipp, M.Ya. Schelev, J.N. Serduchenko and T. Thebault, Rev. Sci. Instrum. in press.

28. G. Zimmerer, HASYLAB, Private Communication.

29. G.V. Marr, I.H. Munro and V. Saile, "The scientific case for the European VUV storage ring", European Science Foundation, Strasbourg, 1981.

30. Part IV Nuc.Instrum.Maths. 177, (1980) 227-270 and references therein.

31. M.W. Poole, "Report on the state of the art in the field of free electron lasers and proposals for their development", European Science Foundation, Strasbourg, 1980.

Figure Captions

Fig.1 A plan of the synchrotron radiation source (SRS) at Daresbury Laboratory and a summary of its operational parameters (from[8]).

Fig.2 The continuous spectrum produced by the SRS from normal bending magnets (1.2 T) and from the wiggler (4.5 T). The spectrum is given for a 1 A 2 GeV stored beam. The intensity at the peak is approximately 5×10^{13} photons per second (from[8]).

Fig.3 The wavelength variation of the angular divergence of radiation from the SRS for a normal 1.2 T bending magnet and at 1.2 T field. The angular divergence is defined to be the full width of the beam between the half intensity values above and below the orbit plane (from[8]).

Fig.4 The geometry associated with the duration of light pulses viewed in a storage ring.

Fig.5 (i) The excitation light pulse from SPEAR seen by an RCA 8850 photomultiplier using the "single photon" method. (ii) Simulated anisotropy decay profiles, using the excitation function in 5(i), calculated using a range of correlation times from 0.1ns to 10ns for an initial anisotropy of 0.2 and decay time of 5ns. Measured anisotropy decay curves for 10μM n-acsetyltryptophanamide in glycerol/water mixtures. The measured slopes (correlation times) of 16.8ns, 0.38ns, <.05ns correspond to the measured solvent viscosities of 1445, 304, 17 and 1.4 cp respectively, from [15].

Fig.6 Measurements of the intensity profile radiated by a single positron bunch in the Stanford storage ring, SPEAR. The visible region bunch shape was observed using an Imacon 600 streak camera triggered when a single positron bunch passed through the source point[18].

Fig.7 Intensity pulse profiles (which are identical for all wavelengths) radiated by a storage ring (from[22]). (i) The signals from a storage ring in the "single bunch" mode have a repetition period determined by the orbit time (T_o) of the ring. (ii) Signals from a "filled" ring have a repetition period (T_{rf}) determined by the radio frequency used for acceleration. (iii) Fluorescence signals which derive from pulses in 7(ii) are delayed slightly and of different shape to the excitation pulses.

Fig.8 A schematic illustration of the Fourier transform of the pulses shown in fig.7(ii). The envelope of the excitation pulse transform $F_I(n)$ is outlined with a continuous line; the envelope of the measured fluorescence decay function transform $F_R(n)$ is shown with a dashed line.

Fig.9 i) The output pulse from the anode of an RCA 8850 photomultiplier tube viewing pulses of radiation from SPEAR (Stanford).

ii) The frequency dependence of the output power from the same photomultiplier tube operating under the same conditions used in (i). The spectrum was measured with the storage ring in the "single bunch" mode.

Fig.10 Phase shift apparatus for measuring time delay at high harmonic frequencies of the storage ring. Phase comparisons are made between a high frequency reference from the storage ring and an optically derived signal obtained with, and without the sample in transmission.

Fig.11 This diagram revels the very limited area in the electromagnetic spectrum (shown lined) which has been used for short time studies. Laser sources have produced data at a few specific wavelengths. In principle, the hope is that the use of synchrotron radiation sources will permit this diagram to be completely filled, at least down to times ~ 1 ps.

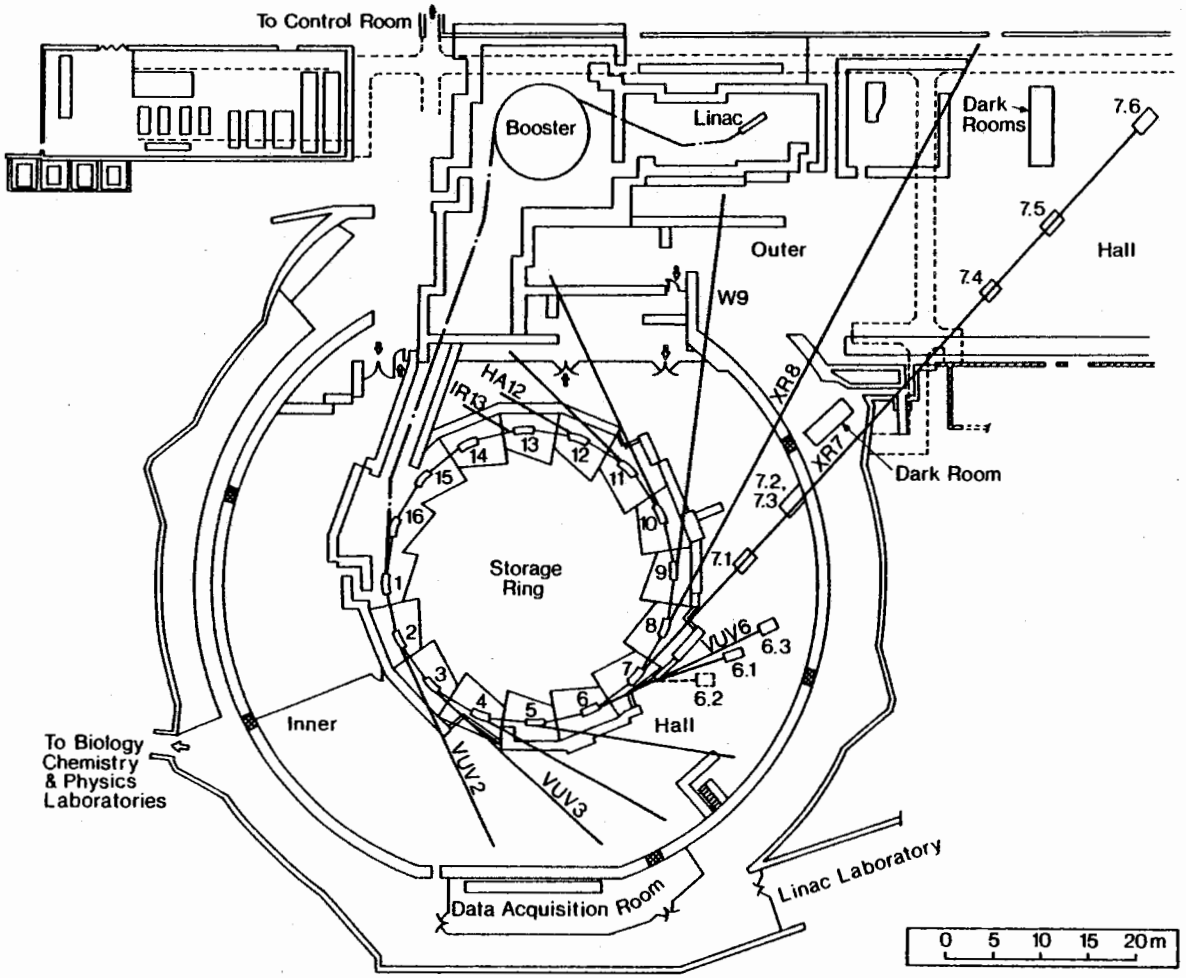
To Control Room
Booster
Linac
Dark Rooms
7.6
7.5
Hall
Outer
7.4
W9
HA12
IR13
XR8
XR7
Dark Room
7.2, 7.3
7.1
Storage Ring
VUV6
6.3
6.1
6.2
Inner
Hall
To Biology Chemistry & Physics Laboratories
VUV2
VUV3
Data Acquisition Room
Linac Laboratory
0 5 10 15 20m

Fig. 1

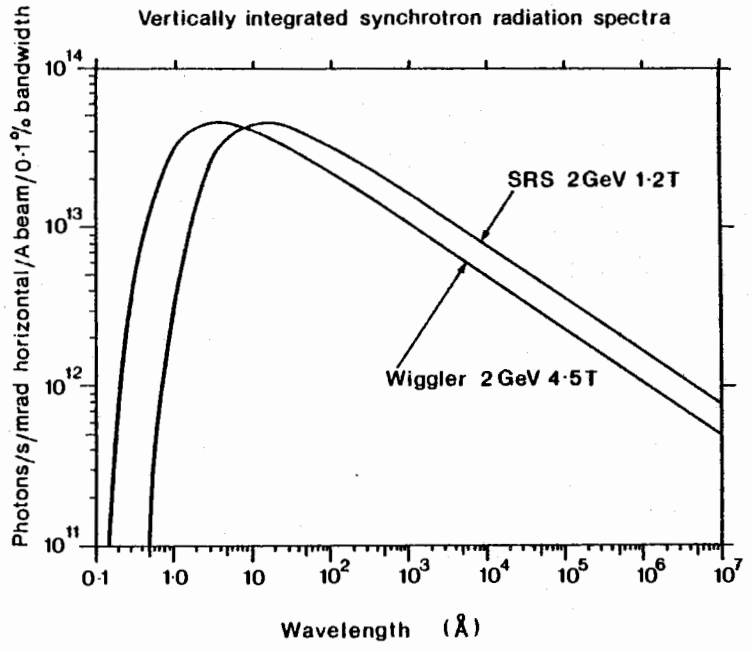
Vertically integrated synchrotron radiation spectra
Photons/s/mrad horizontal/A beam/0·1% bandwidth
SRS 2GeV 1·2T
Wiggler 2GeV 4·5T
Wavelength (Å)

Fig. 2

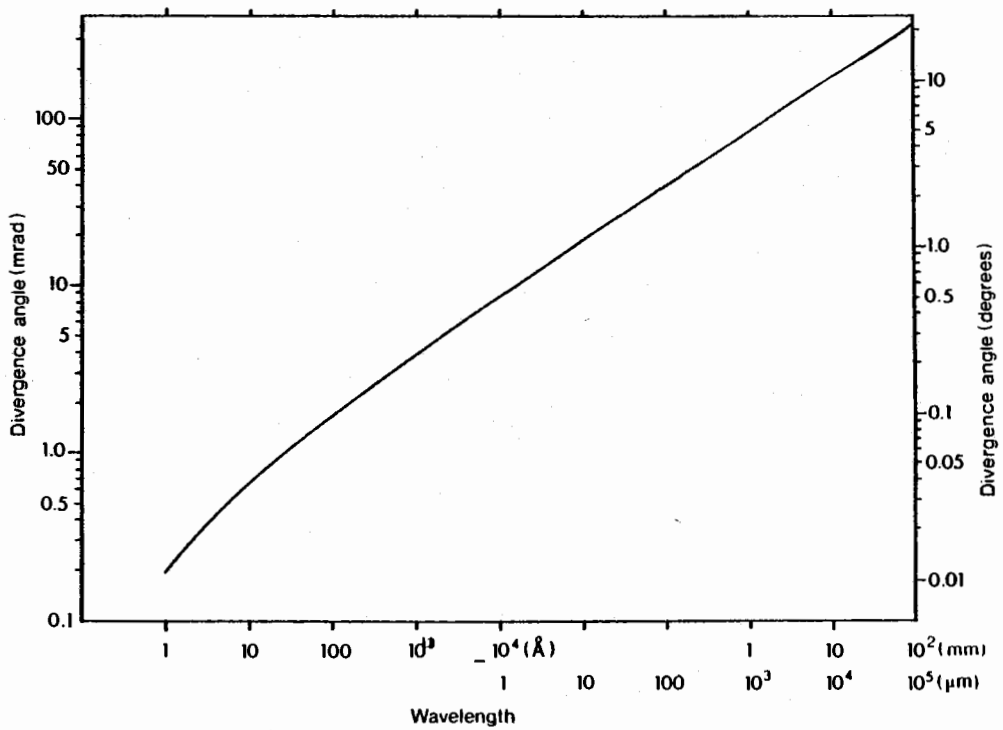
Divergence angle (mrad)
Divergence angle (degrees)
Wavelength

Fig. 3

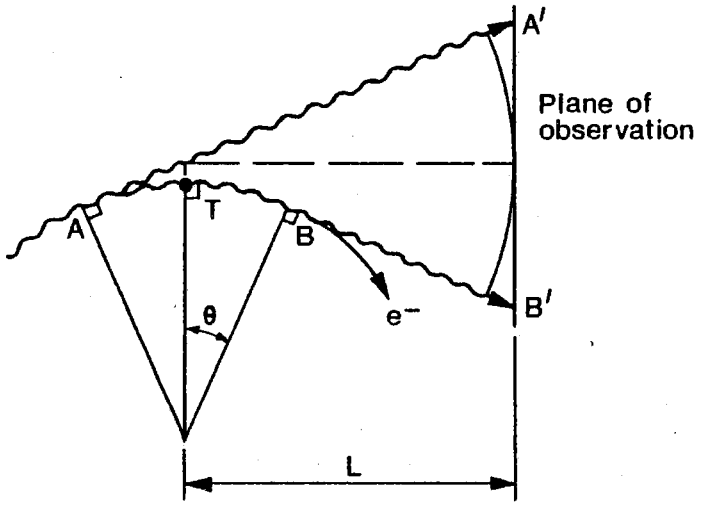
A′
Plane of
observation
A
T
B
B′
θ
e⁻
L

Fig. 4

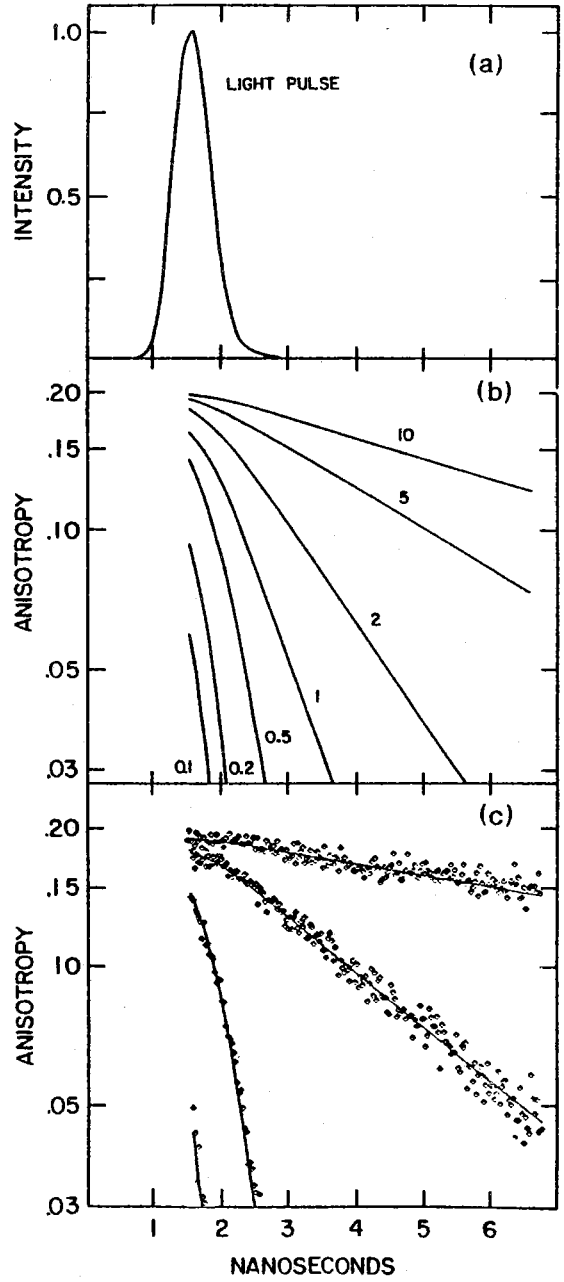
1.0
0.5
INTENSITY
LIGHT PULSE
(a)
.20
.15
.10
.05
.03
ANISOTROPY
(b)
10
5
2
1
0.5
0.2
0.1
.20
.15
.10
.05
.03
ANISOTROPY
(c)
1
2
3
4
5
6
NANOSECONDS

Fig. 5

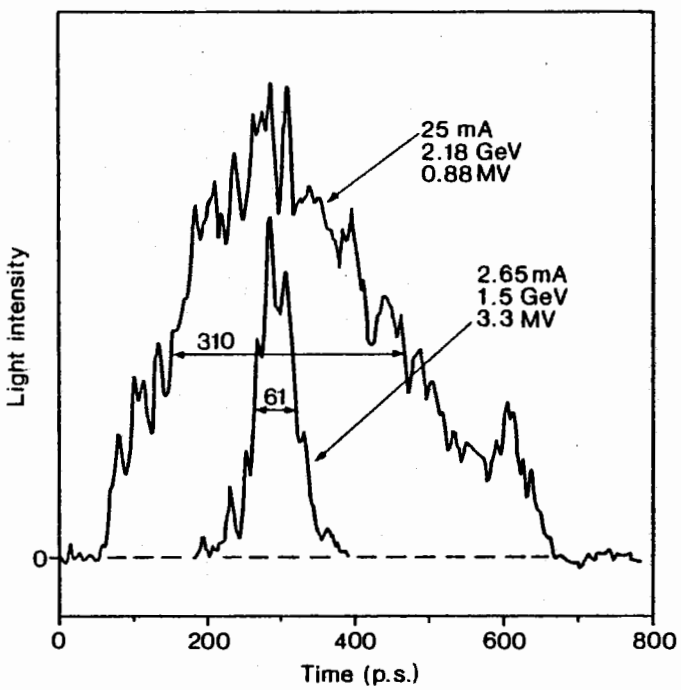
Light intensity
25 mA
2.18 GeV
0.88 MV
2.65 mA
1.5 GeV
3.3 MV
310
61
0
0
200
400
600
800
Time (p.s.)

Fig. 6

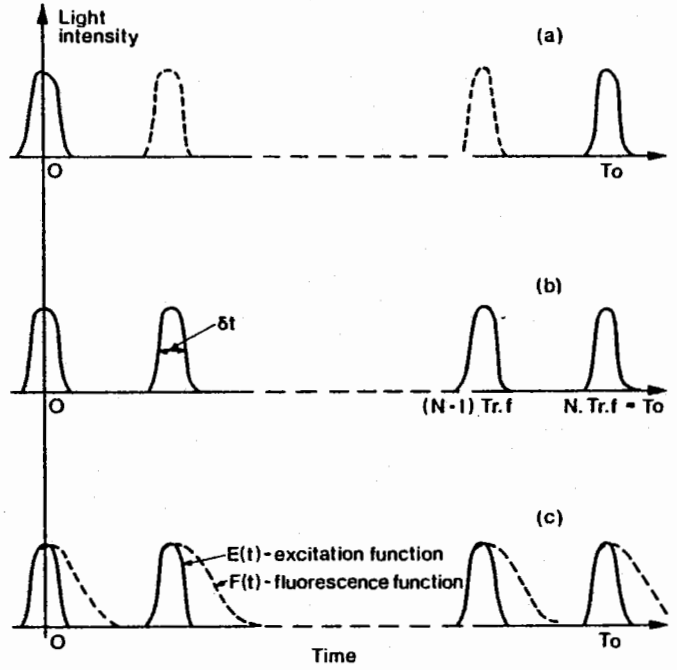
Light intensity
(a)
O
To
(b)
δt
O
(N-1) Tr.f
N. Tr.f = To
(c)
E(t) - excitation function
F(t) - fluorescence function
O
Time
To

Fig. 7

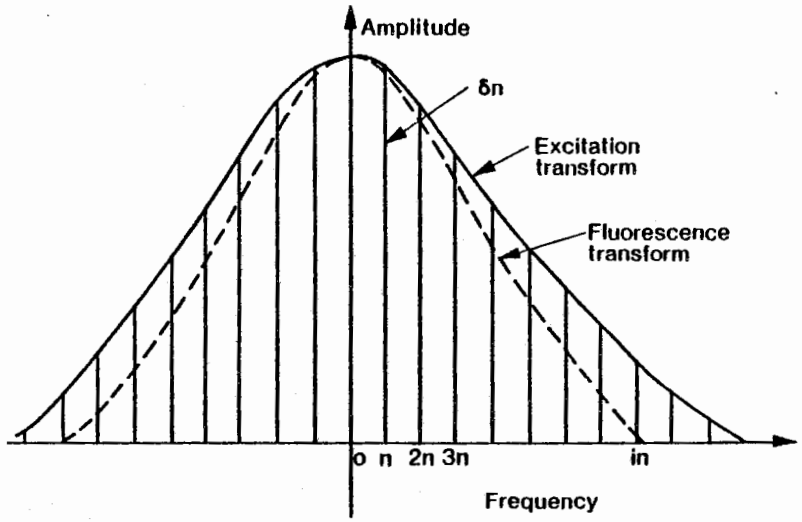
Amplitude
δn
Excitation transform
Fluorescence transform
o n 2n 3n
in
Frequency

Fig. 8

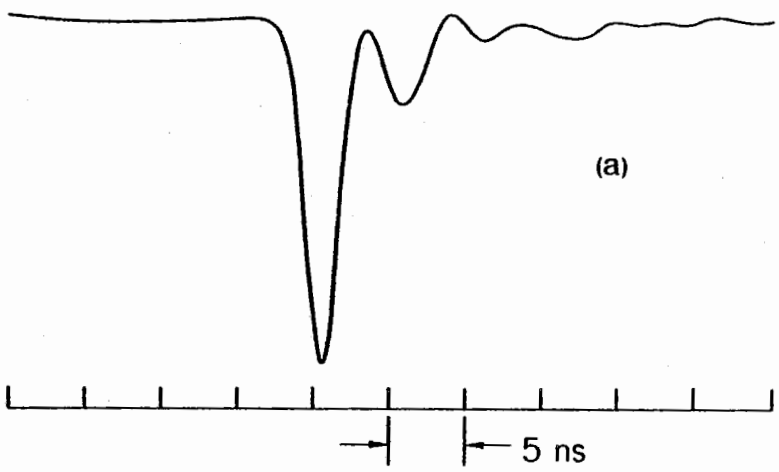
(a)
5 ns

Fig. 9 (a)

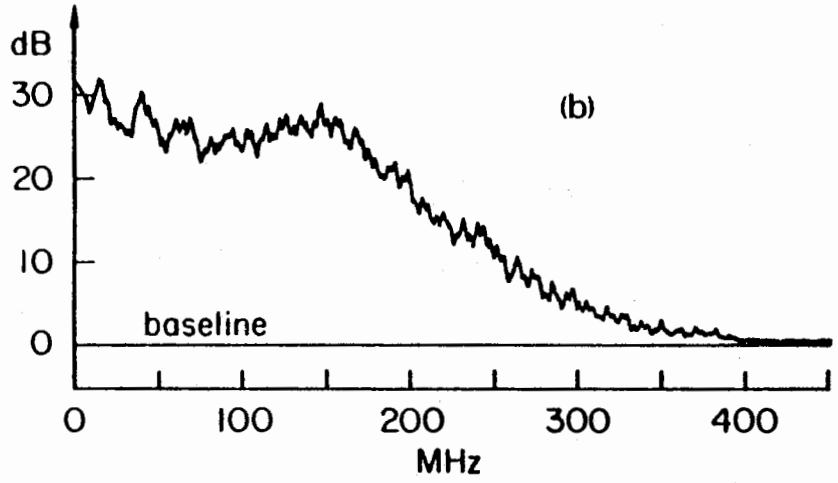
dB
30
20
10
0
(b)
baseline
0
100
200
300
400
MHz

Fig. 9 (b)

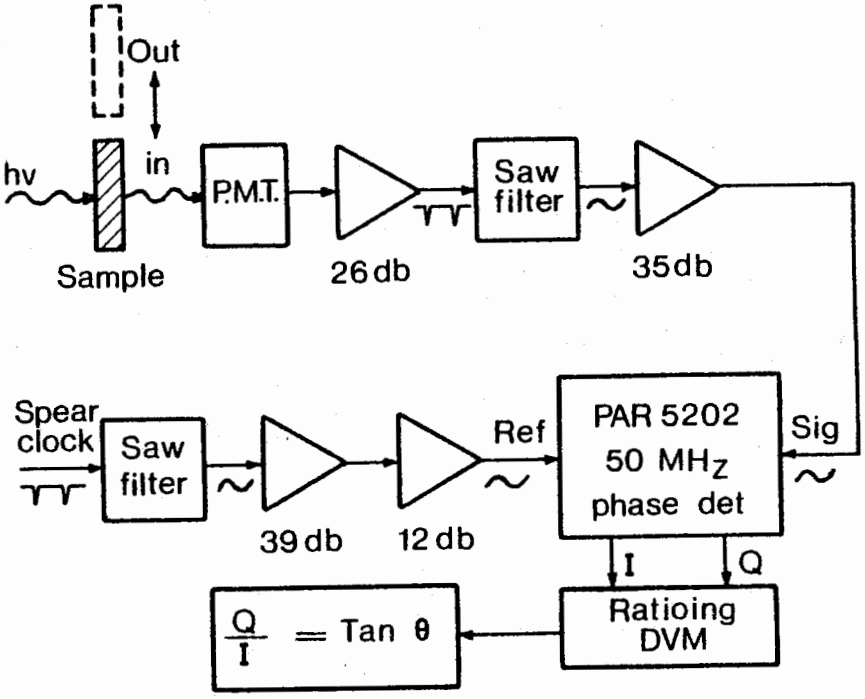
Out
in
hv
P.M.T.
Saw filter
Sample
26 db
35 db
Spear clock
Saw filter
39 db
12 db
Ref
PAR 5202
50 MHz
phase det
Sig
I
Q
Ratioing DVM
Q/I = Tan θ

Fig 10

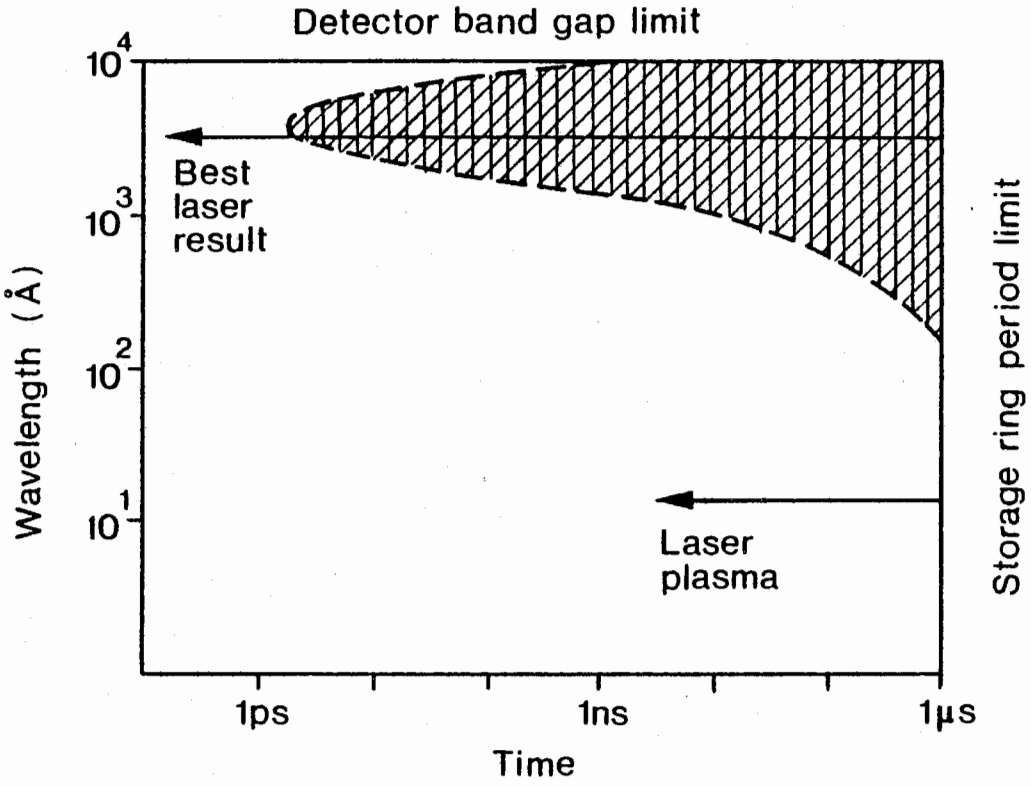
Detector band gap limit
10^4
10^3
10^2
10^1
Wavelength (Å)
Best
laser
result
Laser
plasma
Storage ring period limit
1ps
1ns
1μs
Time

Fig.11